

# Effect of uniform and periodic doping by Ce on the properties of barium strontium titanate thin films

Swaraj Basu · Ankur Verma · D. C. Agrawal ·  
Y. N. Mohapatra · Ram S. Katiyar

Received: 21 October 2005 / Accepted: 12 September 2007 / Published online: 12 October 2007  
© Springer Science + Business Media, LLC 2007

**Abstract** A significant decrease in the dielectric loss and leakage current by introducing Ce in small amounts into BST thin films is demonstrated. The other effects of Ce doping are a lowering of the dielectric constant and a lower temperature coefficient of dielectric constant. In films containing a periodic fluctuation of Ce concentration through the thickness, prepared using a multilayer approach, the dielectric loss is further reduced. The periodicity of the composition is shown to have a significant effect on the properties. The properties of the multilayer films are seen to be significantly different from the single layer films of corresponding average composition.

**Keywords** BST · Thin films · Multilayers ·  
Electrical properties

## 1 Introduction

Electroceramic thin films of materials such as BST (Ba, Sr TiO<sub>3</sub>), have potential applications in capacitor cells of DRAM's (dynamic random access memories), tunable microwave devices, thermal imaging arrays, optoelectronic devices, sensors, etc. It is therefore of great interest to tailor the properties of these materials in the thin film form to suit a desired application. A common way to achieve this has been to dope the material with different alio or homovalent

ions. Properties such as dielectric constant, loss, tunability, leakage current etc. can be significantly altered by such doping.

If the electroceramic is to be used in the thin film form then another approach to tailor the properties becomes available. Rather than using a single film, a film consisting of several thin layers of different materials can be fabricated. It has been found that the properties of such a multilayer structure are a function of the composition, number and thickness of the constituent layers. Very often, properties, much improved as compared to the single layer are obtained. Furthermore, the properties of the multilayers can not at present be predicted from the properties of the individual layers as additional factors such as stresses due to lattice mismatch or thermal history, inter diffusion, etc. come into play leading to unexpected changes in properties.

Y. Ohya et al. [1] studied the temperature dependence of the dielectric constant of the multilayered films of lead titanate (PT) and barium titanate (BT). The dielectric constant of PT as well as BT is a strong function of temperature in the neighborhood of room temperature, an undesirable property. It was observed that the dielectric constant of the multilayers remains almost constant within the measured temperature range. Poyato et al. [2] have also observed a flattening of the dielectric constant with temperature in (Pb,La)TiO<sub>3</sub> (PTL)/(Pb,Ca)TiO<sub>3</sub> (PTC) multilayers and attributed this to lower number of defect dipoles in the multilayer films. Safari et al. [3] observed that BT/BST multilayer thin films show higher dielectric constant than those of pure BT and BST films having the same total thickness of 250 nm. This higher dielectric constant was attributed to the strain between the sublayers. Wang et al. [4] studied multilayered films of PZT of different compositions having tetragonal and rhombohedral phases and found that the dielectric constant of the

S. Basu · A. Verma · D. C. Agrawal (✉) · Y. N. Mohapatra  
Materials Science Program, Indian Institute of Technology,  
Kanpur 208016, India  
e-mail: agrwald@iitk.ac.in

R. S. Katiyar  
Department of Physics, University of Puerto Rico,  
San Juan, PR 00931-3343, USA

multilayered film is five times that of single tetragonal phase PZT film. This high dielectric constant was attributed to the interface effect between tetragonal and rhombohedral phases. Yan et al. [5] found that the fatigue property of lead zirconate titanate (PZT) film improved by inserting BST layers in between PZT film and Pt electrode. D. Bao et al. [6] also found an improvement in the fatigue property by introduction of BLT layers in between PZT film and Pt electrode. These additional layers such as BST and BLT act as oxygen vacancy absorbers and hence improve the fatigue property.

Individual sublayer thickness plays a vital role in modifying the properties of multilayer films. Li et al. [7] observed ultra high dielectric constant in lead magnesium niobate (PMN)/lead zinc niobate (PZN)-PT multilayer films as sublayer thickness approached the nanometer scale. This can be taken as an evidence of high dielectric constant of the interfaces as at this thickness the interfaces between the sublayers become dominant. Wang et al. [8] also found an increase in the dielectric constant of the multilayer films with a decrease in the sublayer thickness. Yoon et al. [9] found that a high dielectric constant and low leakage current could be obtained in BSTM/BST/BSTM multilayered films by adjusting the thickness of the sublayers.

Dielectric response of several perovskites modified by doping with rare earths including Ce has been reported in literature. [10–26]. Ce can exist as  $Ce^{3+}$  or  $Ce^{4+}$  depending on the precursor used and the processing temperature. Ce has been found to improve the dielectric and ferroelectric properties and reduce the leakage current density in the sol-gel prepared PZT thin films. [10] A linear decrease in the Curie temperature of barium titanate up to 8 mol% Ce, (21°C per mol% Ce) has been reported in literature. It is further reported that this decrease takes place when  $Ce^{3+}$  replaces  $Ba^{2+}$  and does not occur if  $Ce^{4+}$  replaces  $Ti^{4+}$  [11]. A broadening of the phase transition and a lowering of the dielectric constant of  $BaTiO_3$  by doping with Ce has also been reported [12]. Similar effects have been observed on doping of  $Ba_{0.5}Sr_{0.5}TiO_3$  films by Ce [13]. The Ce doping has been found to significantly increase the lattice parameter of BST due to the larger ionic size of Ce [14]. Wang et al found a significant reduction in the leakage current in Ce doped  $Ba_{0.5}Sr_{0.5}TiO_3$  films deposited on Nb doped  $SrTiO_3$  substrates by PLD. The reduction of the leakage current was ascribed by them due to Ce existing in the  $Ce^{+3}$  state and acting as an acceptor [15].

In the present work we have investigated the effects of doping BST thin films with Ce and have compared their properties with multilayers of BST and Ce-doped BST. Such a structure produces a film with a periodic variation in the concentration of Ce along the thickness of the film. It is found that the properties of the multilayers are significantly different than the single films of corresponding concentra-

tion of Ce and appreciable improvement in some of the properties (dielectric loss, leakage current, figure of merit) can be obtained by uniform or periodic doping of cerium.

## 2 Experimental

$Ba_{0.8}Sr_{0.2}TiO_3$  (BST) and  $Ba_{0.8}Sr_{0.2}Ce_xTi_{1-x}O_3$  (BSCT) thin films and their multilayers are deposited on Pt/Ti/SiO<sub>2</sub>/Si substrates by sol-gel method. Barium acetate, strontium acetate, cerium nitrate and titanium butoxide are used as starting materials and acetic acid, 2-methoxy ethanol and acetyl acetone are used as solvents/chelating agents for the preparation of the sols [27]. Films are deposited by spin coating at 4000 RPM for 30 s. Each coating is dried at 400°C for 5 minutes followed by firing at 700°C for 10 minutes. This process of coating and firing is repeated several times to get the desired film thickness and the final firing is done at 700°C for 30 minutes. In the single composition films, the value of  $x$  (concentration of Ce) is taken to be 0, 0.002, 0.005, 0.01, 0.02, 0.05 and 0.1. The multilayer films consisted of the configuration [(BST/BSCT)<sub>n</sub>/BST] where  $n$  was taken to be 1, 2 and 4 and the concentration of Ce in the BSCT films was  $x=0.02$  (Fig. 1). Thus the configuration [(BST/BSCT)<sub>4</sub>/BST] consisted of four layers of BSCT and 5 layers of BST. The thickness of each layer was equal and the total thickness of the films, measured by a surface profilometer (Tencor Instruments, model Alfa-Step 100) was held to be constant at 350 nm. Top electrodes of platinum, 0.2 mm in diameter, were deposited on the film through a mask by sputtering. The dielectric constant, loss and C–V measurements were carried out using an impedance analyzer (HP 4192A). I–V measurements were carried out using a Keithley electrometer (model 6517A). For C–V measurements, a step of 0.5 V was applied and the capacitance was recorded at those particular voltages. Similarly, a step of 0.2 V was applied for I–V measurement, and the leakage current was recorded at the corresponding voltages. Low and high temperature measurements were carried out in a vacuum chamber with a liquid nitrogen

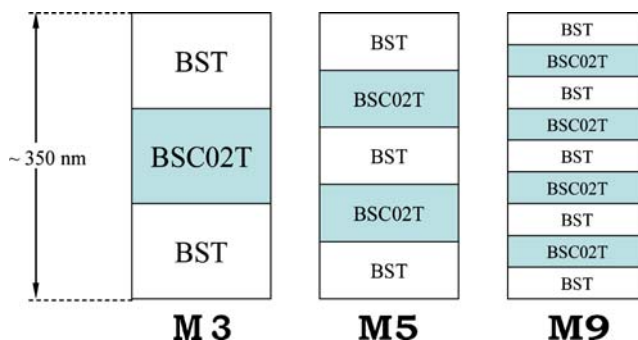


Fig. 1 Schematic showing the arrangement of different layers in the multilayer films

cooled and resistively heated sample stage (M/S Labequip, Chennai).

### 3 Results and discussion

#### 3.1 Uniformly doped films

Figure 2 shows the X-ray diffraction patterns of the BST and the Ce-doped BST films. All the peaks match with the standard peaks of BST. There is slight shift in the peak positions with Ce doping towards smaller angles indicating that the lattice parameter is increasing as the Ce is entering the lattice as reported by Wang et al [14]. No second phase is seen which shows that Ce is soluble in the BST lattice at least up to  $x=0.1$ .

Figure 3 (a) and (b) show the dielectric constant and loss vs frequency for films containing different amounts of cerium. The dielectric constant is seen to decrease as the concentration of Ce,  $x$ , is increased from 0 to 0.1. However, there is an improvement in the dielectric loss with Ce doping, especially at high frequencies. Thus the  $\tan\delta$  values at 1 MHz are very considerably reduced to  $\sim 0.07$  from  $\sim 0.22$  upon doping with 0.02 to 0.1 Ce (Fig. 3(b)). The reductions in the dielectric constant and loss on doping with cerium are in agreement with the results reported for barium titanate [11].

To determine any changes in the structural transition temperatures, the dielectric constant of the films was measured in the temperature range from 150 K to 400 K. In the  $\text{BaTiO}_3$  ceramics there are three transitions on cooling from high temperature: the C→T transition in the temperature range from 393–408 K [28], the T→O transition between 275–280 K and the O→R transition between 180–190 K. Substitution of Ba by isovalent Sr (in

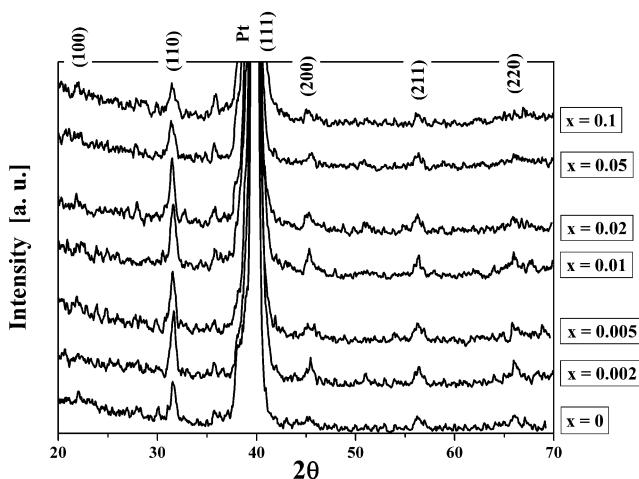


Fig. 2 X-ray diffractograms of films with different Ce contents ( $x=0$  to 0.1)

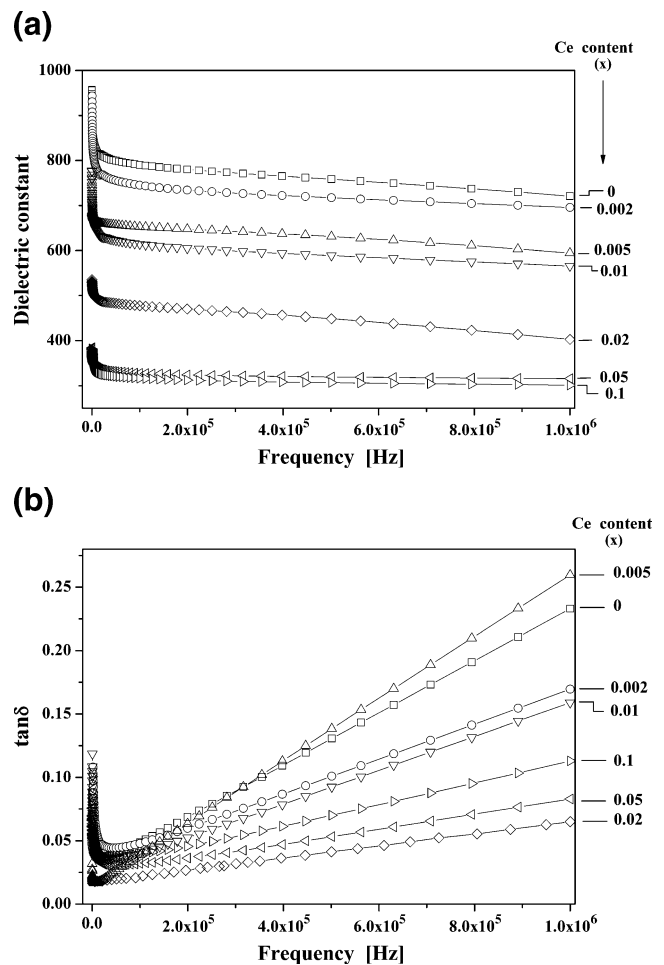
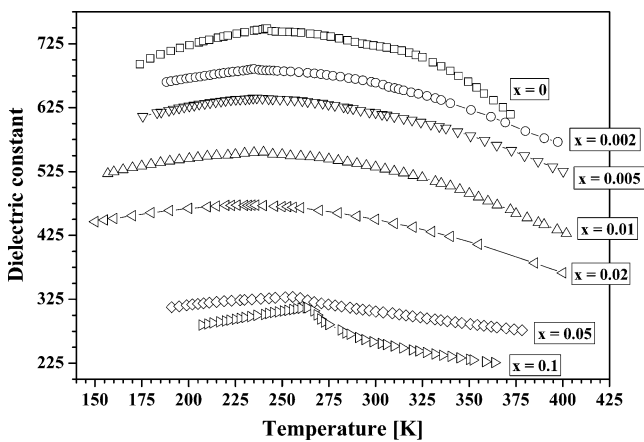


Fig. 3 (a) Dielectric constant vs frequency plots for films with different Ce contents. (b) Loss vs frequency plots for films with different Ce contents

BST) is found to decrease the  $T_C$  (C→T) as well as T→O transition temperatures; however, the temperature corresponding to the O→R transition remains unaffected [29, 30]. The results of the dielectric constant vs. temperature measurement are shown in Fig. 4. The polycrystalline nature of the thin films as well as the retained strain (for example due to the lattice parameter and thermal expansion coefficient mismatch between the film and the underlying substrate) often mask the dielectric anomalies associated with the structural transitions. Even though the  $\text{Ba}_{0.8}\text{Sr}_{0.2}\text{TiO}_3$  thin film ( $x=0$ ) is ferroelectric at room temperature [31, 32], only a broad dielectric anomaly is seen and unlike the bulk counterpart the transition temperatures corresponding to the structural changes are not easily discernible. However, three kink like features are seen at  $\sim 330$ ,  $\sim 285$  and 242 K which can be taken to correspond to the C→T, T→O and O→R transitions. From Fig. 4 it is also clear that the room temperature dielectric constant decreases and the diffuseness of the dielectric anomaly increases with an increase in Ce contents. The kink like



**Fig. 4** Dielectric constant vs temperature at 100 kHz for films with different Ce contents

features at first become weaker as the cerium content is increased to  $x=0.02$  indicating that the phase transitions become smeared as the concentration of cerium is increased. This is in agreement with the observation that the sharp ferroelectric transition in barium titanate becomes diffuse on doping with Ce [11]. This behaviour has been observed with other dopants also [33]. On further increasing the concentration of Ce, a marked kink again appears for  $x=0.05$  and  $x=0.1$  (Fig. 4) at 255 K and 264 K respectively. Hence it appears that, as observed with other dopants, the C→T transition is lowered and the T→O transition temperature is raised so that both the transitions tend to merge.

In many cases, when a non-relaxor ferroelectric is heavily doped with a dopant, a relaxor like behavior characterized by a shift in the temperature of dielectric maximum to higher value with increasing frequency is observed. For example, the onset of such relaxation behavior was observed on replacement of titanium by zirconium to the extent of 35 mole percent in  $\text{Ba}_{0.8}\text{Sr}_{0.2}\text{TiO}_3$  [33]. However, as shown in Fig. 5 (a) and (b), there is no shift in the temperature of dielectric maximum in the Ce doped samples indicating that no relaxor like features develop in BST by doping with up to 0.1 Ce, though, it is possible that the relaxor like features may appear at a concentration higher than those used here.

The leakage current behavior is an important characteristic of dielectric thin films. The films should have a low leakage current at high electric fields. Introduction of a small amount of Ce is found to significantly increase the value of the maximum field up to which a low level of leakage current continues to be maintained. Figure 6 shows the I–V plots of the thin films with different Ce contents. All the curves have two regions—one with a low, constant leakage current and the other in which the leakage current increases rapidly. Small additions of Ce have a dramatic effect on the leakage current. At high fields ( $>18 \text{ MVm}^{-1}$ ),

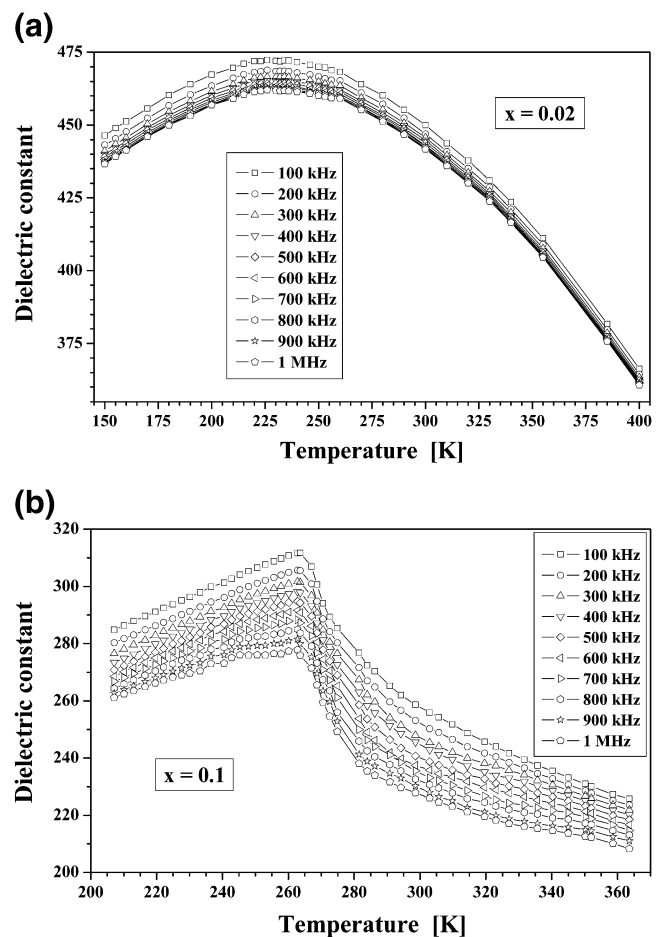


**Fig. 5** (a) Dielectric constant vs temperature for the film with  $x=0.02$  at different frequencies. (b) Dielectric constant vs temperature for the film with  $x=0.1$  at different frequencies

the leakage current is considerably reduced for small additions of Ce up to 0.005, beyond which the leakage current again increases. However, at low fields, the leakage current is higher for  $x=0.002$  but decreases to below that of the undoped film for  $x=0.005$ ; a further increase in the Ce

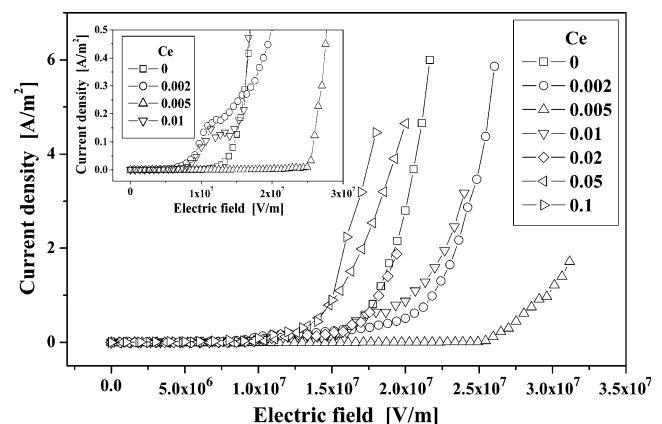


**Fig. 6** Current density vs electric field (I–V) plots for films with different Ce contents

content leads to a progressive increase in the leakage current. Thus the additions of small amounts of Ce ( $x=0.005$ ) are found to be beneficial in significantly lowering the leakage currents in the BST thin films.

The leakage current in the BST thin films is usually analyzed in terms of two groups of mechanisms—interface limited such as Schottky emission or bulk limited which include space charge limited current, Poole–Frenkel mechanism and the hopping conduction mechanism [34, 35]. As discussed later, in the multilayer films also, there are significant changes in the leakage current with the multilayer configuration. In these multilayer films, the electrode–film interface is unchanged so that the changes in the leakage current are not likely to be due to any phenomena occurring at the film–electrode interface. Hence the most likely causes for the changes in the leakage current in the Ce doped films appears to be related to the changes in the bulk of the film such as the pinning of the oxygen vacancies by Ce [36], or the change in the charge distribution inside the film due to the Ce existing in a multivalent state [37],  $Ce^{4+}$  as well as  $Ce^{3+}$ .

The dielectric constant vs. electric field (C–V) characteristics of the thin films is shown in Fig. 7. The hysteresis in the plots on going from the negative field to positive and back is usually taken as an indication of the ferroelectric nature of the film. However, this hysteresis is quite small for the BST film which is known to be ferroelectric and is much larger in the Ce doped films, especially those with small Ce contents (0.002 to 0.01) as indicated by the opening up of the loops in these films. As discussed earlier, the cubic to tetragonal transition temperatures are found to be lowered in the Ce doped films (Fig. 4). Hence, the origin of the hysteresis in the Ce doped films does not appear to be an increased ferroelectric nature but rather due to the movement of ions or charges at the interfaces between the dielectric and the Pt electrode [38].

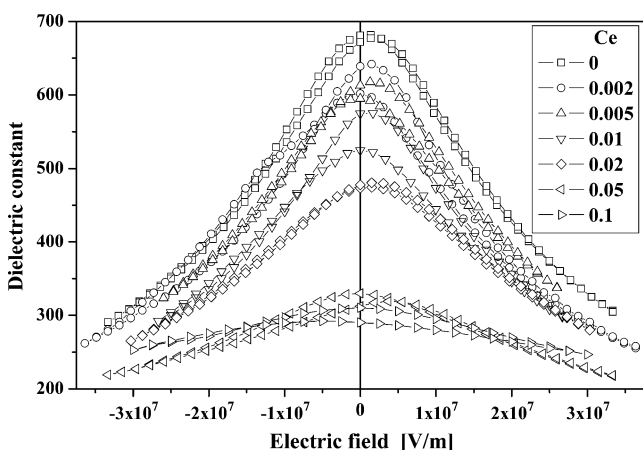


Fig. 7 Dielectric constant vs electric field (C–V) plots for films with different Ce contents

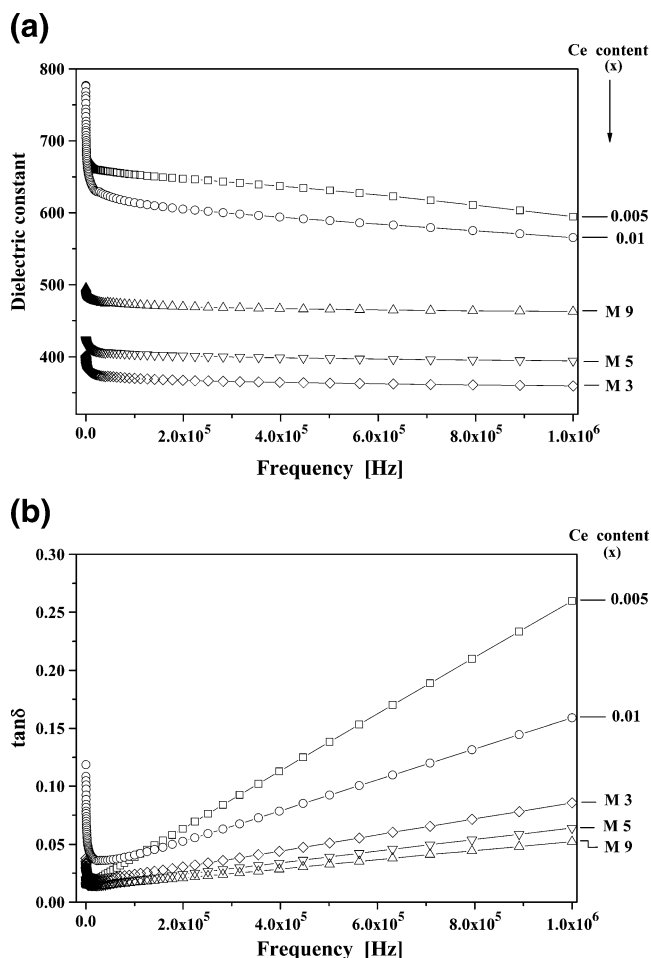
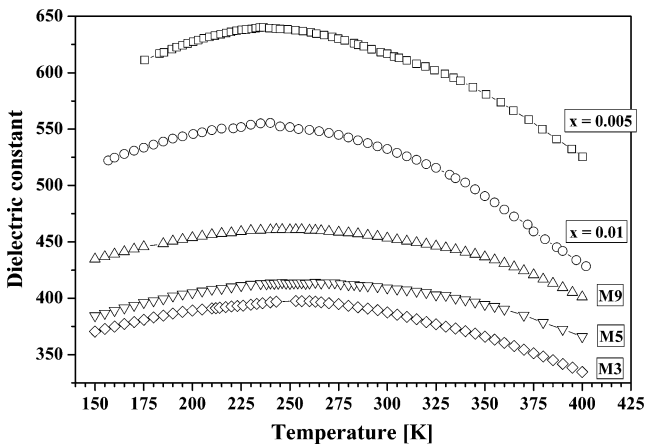


Fig. 8 (a) Dielectric constant vs frequency plots for the multilayer films; the average composition of the multilayer films falls in the range between  $x=0.005$  to  $x=0.01$  of the single layer films, the data for which is also included. (b) Loss vs frequency plots for the multilayer films; the data for single layer films with compositions  $x=0.005$  and  $x=0.01$  is also included for comparison

### 3.2 Multilayer films

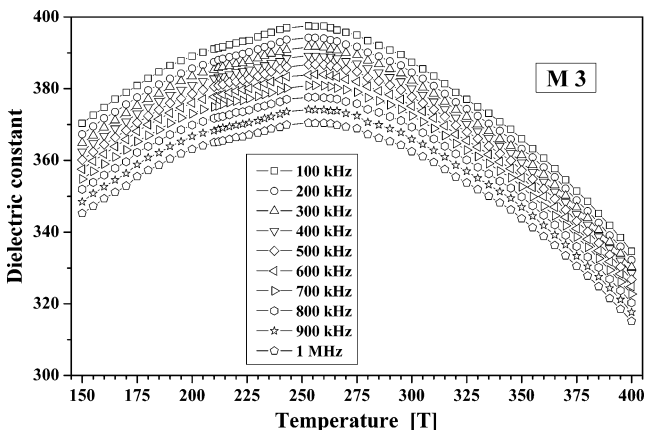
As described earlier (section 2), three configurations of the multilayers were prepared consisting of 1, 2 and 4 layers of BSCT ( $Ba_{0.8}Sr_{0.2}Ce_{0.02}Ti_{0.98}O_3$ ) alternating with 2, 3 and 5 layers of BST ( $Ba_{0.8}Sr_{0.2}TiO_3$ ), all of equal thickness. The total film thickness was maintained at 350 nm with BST layers always in contact with the electrodes. The samples are designated M3, M5 and M9 according to the total number of layers. The calculated average composition in the thin films comes out to be  $x=0.0067$ , 0.008 and 0.0082 respectively which all lie between 0.005 and 0.01, the compositions of two of the single layer films with which the results will be compared.

Figure 8 (a) and (b) show the dielectric constant and loss vs frequency for the different multilayer films; the data for the single layer film with  $x=0.005$  and 0.01 is also included for comparison. It is seen that the multilayers show



**Fig. 9** Dielectric constant vs temperature plot for the multilayer films; the data for single layer films with compositions  $x=0.005$  and  $x=0.01$  is also included for comparison

distinctly lower dielectric constant as compared to single layer samples with the corresponding average composition. Amongst the multilayers, M9 has the highest and M3 has the lowest dielectric constant. If the multilayers are modeled as a series combination of capacitances from the individual layers then their dielectric constant can be calculated using the dielectric data for the single layer films with  $x=0$  and  $x=0.02$  (Fig. 3). Such calculated values are much higher than the measured values, e.g. at 100 kHz the calculated values for the samples M3, M5 and M9 are 649, 626 and 612 while the measured values are 370, 404 and 472 respectively. The films are heated to high temperature (700°C) during preparation. Hence some homogenization of composition through the thickness of the multilayer films is expected. This phenomenon is expected to be most pronounced for the multilayer with the smallest individual layer thickness (i.e. M9) due to small distances over which the transport of cerium by diffusion is required. Hence the dielectric data for M9



**Fig. 10** Dielectric constant vs temperature plot for the multilayer sample M3 at different frequencies

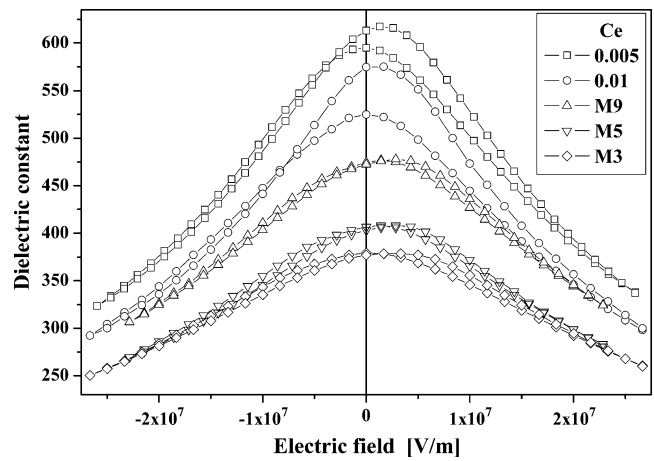


**Fig. 11** Dielectric constant vs electric field (C–V) plot for the multilayer film; the data for single layer films with compositions  $x=0.005$  and  $x=0.01$  is also included for comparison

should be closest to the data for the average composition. Here, that trend is followed; nevertheless the dielectric constant of the multilayers is still considerably less than that of the single layers.

In most of the cases reported in the literature, the dielectric constant of the multilayers is found to be higher than that of any of the constituent layers, as discussed in the Introduction. This is usually ascribed to the presence of a stress in the film due to mismatch at the interfaces or due to a high dielectric constant of the interface. In the present case, the dielectric constant of the multilayers is smaller than that of the corresponding single composition film. It may be because of the formation of a low dielectric constant interface between the different layers. Such interfaces may form due to pinning of the oxygen vacancies by the Ce [36].

**Table 1** Tunability and figure of merit for single layer and multilayer films.

	Dielectric constant	Tan $\delta$	Percent tunability	$K$ factor
<b>a. Ce doped films</b>				
Ce content ( $x$ )				
0	790	0.033	41	12.5
0.002	745	0.048	49	10.2
0.005	653	0.039	38	9.8
0.01	614	0.041	48	10.2
0.02	478	0.058	34	5.9
0.05	328	0.032	31	9.6
<b>b. Multilayer films</b>				
M9	472	0.017	32	18.6
M5	404	0.019	30	16
M3	370	0.024	31	13

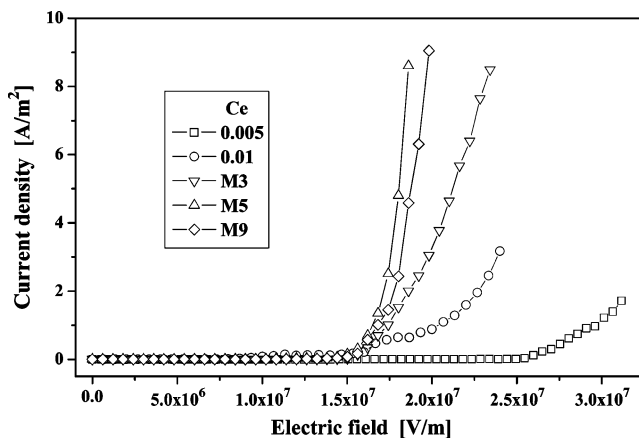


**Fig. 12** Current density vs electric field (I–V) plot for the multilayer films; the data for single layer films with compositions  $x=0.005$  and  $x=0.01$  is also included for comparison

The dielectric loss in the multilayers is much lower as compared to the single films of corresponding compositions especially at frequencies  $>20$  kHz (Fig. 8(b)). The M9 has the lowest while the M3 has the highest loss at all frequencies. The reduced dielectric loss is an advantageous feature for the multilayers. This shows that the use of the multilayer configuration provides an additional variable, in addition to the amount of dopant, to control the properties of the film.

Figure 9 compares the variation in dielectric constant measured at 100 kHz with temperature for the multilayer films with the data for films of corresponding average cerium contents ( $x=0.005$  and  $0.01$ ). The dielectric constant of the multilayers is lower than that of the corresponding average composition at all temperatures. However, a remarkable feature is that the curves become flatter as the number of sublayers is increased. In most applications a low coefficient of variation of the dielectric constant with temperature is desirable. One of the undesirable features of BT and BST films is their strong sensitivity to temperature variation near room temperature. By using the multilayers, this variation may be considerably reduced.

Figure 10 shows the dispersion in dielectric constant with measuring frequency at different temperatures for the M3 sample. The dielectric constant decreases at all temperatures with increasing measurement frequency. However, there is no change in the temperature of maximum dielectric constant on changing the frequency. Similar behaviour was observed for all the other multilayers indicating that no relaxor like behavior develops in the multilayers.

Figure 11 shows the dielectric constant vs electric field (C–V) plots for the multilayer films and the single layer films in the comparable composition range. The plots for the multilayer films are depressed and the loop is much less open as compared to the single layer films. The dielectric

tunability, defined as  $[(C_0 - C_V)/C_0] \times 100$ , where  $C_0$  is the capacitance at zero voltage and  $C_V$  is the same at a voltage  $V$  and the figure of merit,  $K$ , defined as the tunability divided by the loss tangent were calculated from the C–V plots and are given in Table 1. The tunability of the single layer films is between 30–50 and tends to decrease as the Ce content is increased. The tunability of the multilayer films is about 30. These figures are calculated using the value of  $C_V$  at 8 volts; use of a higher voltage would yield higher numbers. Although the tunability of the multilayers is on the lower side, the  $K$  factor is much higher as compared to the single layer films due to their much lower dielectric loss—the  $K$  factor for the multilayers is between 13–18 as compared to 6–12 for the single layer films. Interposing the Ce doped layers between layers of BST thus increases the figure of merit significantly from 12 to 18.

The I–V characteristics of the multilayers are not so attractive (Fig. 12)—the leakage currents in the multilayer films are higher than those in the single layer films of comparable Ce content and the leakage current increases as the number of layers increases i.e. it diverts more and more from the value for the single layer film as the gradient in Ce becomes smaller which is an unexpected result and needs to be further investigated.

#### 4 Summary

Doping of BST thin films of composition  $\text{Ba}_{0.8}\text{Sr}_{0.2}\text{TiO}_3$  with Ce has been carried out. The films had either a uniform distribution of Ce or had a periodic fluctuation in the Ce concentration through the thickness of the film. The latter were prepared by depositing alternate layers of BST and Ce doped BST. The introduction of Ce generally results in a reduction in the dielectric loss of the films; the dielectric constant is also reduced. A significant reduction in the leakage current is observed when the films are doped with a small amount ( $x=0.005$ ) of Ce. The various structural transitions, as observed by measuring the dielectric constant as function of temperature, are smeared as the Ce content first increases but then a sharp transition is seen to be present in the films containing higher amount ( $x=0.05$  and  $x=0.1$ ) of Ce.

A further significant decrease in the dielectric loss is observed in the multilayer films with periodic fluctuation in the concentration of Ce. The dielectric constant of these films is lower than expected from a series capacitor model indicating the formation of low dielectric constant layers at the interfaces of the layers. The C–V results show that the quality factor of the BST films can be significantly improved by interposing a single layer of Ce doped composition between the two BST layers.

**Acknowledgements** Support, in part, by the Government of India through grant Nos. ERIP/ER/0300199/M01 and DST/INT/US (NSF-RP052)/2000 and by NSF through NSF-DMR-305588 is greatly acknowledged.

## References

1. Y. Ohya, T. Ito, Y. Takahashi, *Jpn. J. Appl. Phys.* **33**, 5272–5276 (1994)
2. R. Poyato, M.L. Calzada, L. Pardo, *J. Appl. Phys.* **97**, 034108 (2005)
3. A. Safari, R.K. Panda, V.F. Janas, in *Advanced Ceramic Materials: Key Engineering Materials*, vols. 122–124, ed. by M. Mostaghani (Trans Tech Publications, 1996), pp. 35–71
4. C. Wang, Q.F. Fang, Z.G. Zhu, A.Q. Jiang, S.Y. Wang, B.L. Chen, Z.H. Chen, *Appl. Phys. Lett.* **82**(17), 2880–2882 (2003)
5. F. Yan, Y. Wang, H.L.W. Chen, C.L. Choy, *Appl. Phys. Lett.* **82**(24), 4325–4327 (2003)
6. D. Bao, N. Wakiya, K. Shinozaki, N. Mizutani, *Ferroelectrics* **220**, 27–32 (2002)
7. K. Li, K. Zou, Y. Wang, H. Jiang, X. Chen, *Mater. Res. Soc. Symp. Proc.* **784**, C 8.9.1–C 8.9.6 (2004)
8. C. Wang, B.L. Cheng, S.Y. Wang, H.B. Lu, Y.L. Zhuo, Z.H. Chen, G.Z. Wang, *Appl. Phys. Lett.* **84**(5), 765–767 (2004)
9. K.H. Yoon, J.C. Lee, J. Park, D.H. Kang, C.M. Song, Y.G. Seo, *Jpn. J. Appl. Phys.* **40**, 5497–5500 (2001)
10. S.B. Majumder, D.C. Agrawal, Y.N. Mohapatra, R.S. Katiyar, *Math. Sci. Eng.* **B98**, 25–32 (2003)
11. M. Cernea, O. Monnereau, P. Llewellyn, L. Tortet, C. Galassi, *J. Eur. Ceram. Soc.* **26**, 3241–3246 (2006)
12. D.-Y. Lu, X.-Y. Sun, M. Toda, *J. Phys. Chem. Solids* **68**, 650–664 (2007)
13. Z. Yu, C. Ang, Z. Jing, P.M. Vilarinho, J.L. Baptista, *J. Phys. Condens. Matter* **9**, 3081 (1997)
14. S.Y. Wang, B.L. Cheng, C. Wang, S.Y. Dai, K.J. Jin, Y.L. Zhou, H.B. Lu, Z.H. Chen, G.Z. Yang, *J. Appl. Phys.* **99**, 013504 (2006)
15. S.Y. Wang, B.L. Cheng, C. Wang, S.A.T. Redfern, S.Y. Dai, K.J. Jin, H.B. Lu, Y.L. Zhou, Z.H. Chen, G.Z. Yang, *J. Phys. D: Appl. Phys.* **38**, 2253–2257 (2005)
16. F.D. Morrison, D.C. Sinclair, A.R. West, *J. Appl. Phys.* **86**, 6355–6366 (1999)
17. D.F.K. Hennings, B. Schreinemacher, H. Schreinemacher, *J. Eur. Ceram. Soc.* **13**, 81–88 (1994)
18. D. Makovec, D. Kolar, *J. Am. Ceram. Soc.* **80**, 45–52 (1997)
19. J. Zhi, Y. Zhi, A. Chen, *J. Mater. Res.* **17**, 2787–2793 (2002)
20. A.S. Shaikh, R.W. Vest, *J. Am. Ceram. Soc.* **69**, 689–694 (1986)
21. T.R.N. Kutty, P. Murugaraj, *J. Mater. Sci.* **22**, 3652–3664 (1987)
22. Y. Park, H.G. Kim, *Jpn. J. Appl. Phys. Part 1* **36**, 3558–3563 (1997)
23. Y. Park, H.G. Kim, *Ferroelectrics* **198**, 67–76 (1997)
24. D.-Y. Lu, T. Koda, H. Suzuki, M. Toda, *J. Ceram. Soc. Jpn.* **113**, 721–727 (2005)
25. M.A.A. Issa, N.M. Molokhia, S.A. Nasser, *J. Phys. D* **17**, 571–578 (1984)
26. Y. Park, K. Cho, H.G. Kim, *J. Am. Ceram. Soc.* **81**, 1893–1899 (1998)
27. G. Burns, F.H. Dacol, *Phys. Rev.* **B28**, 2527 (1983)
28. Z. Kutnjak, C. Filipic, R. Pirc, A. Levstik, *Phys. Rev. B* **59**, 294 (1999)
29. B. Jaffe, W.R. Cook, H. Jaffe, *Piezoelectric Ceramics* (Academic Press, London, 1971)
30. F. John, G. Shirane, *Ferroelectric Crystals* (Pergamon, New York, 1962)
31. J.G. Cheng, X. Meng, B.J. Tang, S. Guo, Z. Wang, *Appl. Phys. Lett.* **75**, 2132 (1999)
32. F.M. Pontes, *J. Appl. Phys.* **91**, 5972 (2002)
33. Anju Dixit, Santosh K. Gupta, D. C. Agrawal, Y. N. Mohapatra, S. B. Majumder, and R. S. Katiyar. (Communicated).
34. Y.B. Lin, J.Y. Lee, *J. Appl. Phys.* **87**, 1841 (2000)
35. H. Schroeder, S. Schmitz, P. Meuffels, *Appl. Phys. Lett.* **82**, 781 (2003)
36. S.B. Majumder, Y.N. Mohapatra, D.C. Agrawal, *Appl. Phys. Lett.* **70**, 138 (1997)
37. A. Garg, D.C. Agrawal, *J. Mater. Sci. Mater. Electron.* **10**, 649–652 (1999)
38. M. Izuha, K. Abe, N. Fukushima, *Jpn. J. Appl. Phys.* **36**, 5866 (1997)